Chin. J. Mech. Eng. (2017) 30:241–255
DOI 10.1007/s10033-017-0074-8

ORIGINAL ARTICLE

Magnetostrictive and Kinematic Model Considering the Dynamic Hysteresis and Energy Loss for GMA

Huifang LIU[1] · Xingwei SUN[1] · Yifei GAO[1] · Hanyu WANG[1] · Zijin GAO[1]

Received: 14 March 2016 / Revised: 5 August 2016 / Accepted: 2 September 2016 / Published online: 21 March 2017

Abstract Due to the influence of magnetic hysteresis and energy loss inherent in giant magnetostrictive materials (GMM), output displacement accuracy of giant magnetostrictive actuator (GMA) can not meet the precision and ultra precision machining. Using a GMM rod as the core driving element, a GMA which may be used in the field of precision and ultra precision drive engineering is designed through modular design method. Based on the Armstrong theory and elastic Gibbs free energy theory, a nonlinear magnetostriction model which considers magnetic hysteresis and energy loss characteristics is established. Moreover, the mechanical system differential equation model for GMA is established by utilizing D'Alembert's principle. Experimental results show that the model can preferably predict magnetization property, magnetic potential orientation, energy loss for GMM. It is also able to describe magnetostrictive elongation and output displacement of GMA. Research results will provide a theoretical basis for solving the dynamic magnetic hysteresis, energy loss and working precision for GMA fundamentally.

Keywords Giant magnetostrictive actuator · Kinematic model · Magnetostrictive model · Magnetic hysteresis · Energy loss

1 Introduction

By right of its excellent characteristics of large magnetostrictive coefficient at room temperature (1500×10^{-6}–2000×10^{-6}), high energy density, low magnetic field drive, high magneto mechanical conversion efficiency, and fast response speed etc., giant magnetostrictive materials (GMM) and its applications have attracted wide attention at home and in abroad academic circles and industrial community. This kind of material has two important physical effects: strong magnetostrictive effect and inverse magnetostrictive effect [1]. Magnetostrictive effect can be used to produce driving device and the inverse magnetostrictive effect can be use to develop force or strain sensor.

Giant magnetostrictive actuator (GMA) is a new generation of drive device and it has features such as great output force, relatively smooth frequency response, wide range of temperature, maneuverability with low voltage, and accurate control [2]. GMA have been applied to precision and ultra-precision machining, linear motor, sonar system, astronomy, medicine and other fields [3–8]. Magnetic hysteresis and eddy-current heating are the most significant disadvantages in GMM [9, 10]. Displacement precision of GMA is affected by the magnetic hysteresis characteristic, eddy-current energy loss and other energy loss seriously [11, 12]. Mostly, GMM's magnetic hysteresis is compensated and GMA's working accuracy is improved through an effective control method usually whose response speed is fast and precision is high. However, to solve hysteresis and accuracy problems

Supported by National Natural Science Foundation of China (Grant No. 51305277), Doctoral Program of Higher Education China (Grant No. 20132102120007), Shenyang Science and Technology Plan Project (Grant No.F15-199-1-14), and China Postdoctoral Science Foundation (Grant No.2014T70261).

✉ Xingwei SUN
sunxingw@126.com

[1] School of Mechanical Engineering, Shenyang University of Technology, Shenyang 110870, China

fundamentally, the key points are establishing a mathematical model which can describe and explain the magnetization hysteresis process and energy loss characteristics in essence.

Currently, there are primarily four kinds of models to describe magnetic hysteresis phenomenon for GMM: linear magnetomechanical constitutive equations, Maxwell model, J-A magnetization theory, Preisach model. The coupled linear magnetomechanical constitutive equations are widely applied in describing giant magnetostrictive displacement [13]. It is helpful to understand the working principle of GMM and GMA. However, the model does not consider nonlinearity characteristics and magnetic hysteresis of material, thus it is only suitable for describing the working process of GMA under low static magnetic field. Maxwell model is a model based on the energy conversion and hysteresis mechanism for the condition that operating frequency is much lower than first natural vibration frequency of the actuator system, especially for the analogue simulation of magnetic hysteresis phenomenon. J-A model is a magnetization model built on the basis of the domain theory, which not only can clearly disclose the mechanism of material's magnetization process but also can analyze the coupling effect between magnetization and magnetostriction. But it only reflects the specific magnetization process and the composition of magnetization for GMM. It is not able to reflect the energy loss problem [14]. Preisach model is a universal mathematical model to describe the hysteresis phenomenon based on the multi-valued function operator [15, 16]. In recent years, Preisach model has been widely adopted in model and control for various kinds of hysteresis system relying on its good nonlinear hysteresis predictability, good adaptability and other merits [17]. Based on the classical Preisach model, Bergqvist and Engdahl established a stress-dependent magnetic Preisach hysteretic model [18] and TAN et al. established a dynamic hysteresis nonlinear model for linear systems [19]. However, since it is a black-box model based on experimental data, it cannot reveal the mechanism of hysteresis magnetization process and energy loss in essence. Therefore, in order to improve the working precision and repeatability fundamentally, an effective model must be established which can consider the hysteresis and energy loss existing in magnetization process.

In this paper, a GMA which uses GMM rod as the driving element is presented. The design process adopts modular design method. Furthermore, on the basis of Armstrong theory and through analyzing the composition of GMM's elastic Gibbs free energy, a nonlinear magnetization and magnetostriction model which considers magnetic hysteresis and energy loss characteristics is established. Through analyzing GMA's mechanical system, a mechanical system differential equation model and transfer function model for GMA are deduced utilizing D'Alembert's principle. Finally, GMA's mechanical system model and GMM's magnetization and magnetostrictive model are combined together, and an output displacement model which considers the magnetic hysteresis and energy loss characteristics is gotten for the GMA involved in this paper.

The paper is organized as follows. In section 2, the working principle and GMA structure are expounded. In section 3, a mathematical model which considers magnetic hysteresis and energy loss is established for the GMA. In section 4, there is a comparison between the results of model and experiment, which verifies the model validity. Moreover, GMM's magnetization characteristic, energy loss characteristic and working performance of GMA are studied by experiment and model simulation technology. Finally, some conclusions are remarked in section 5.

2 Structure and Working Principle of GMA

The main principle of GMA is utilizing magnetostrictive effect occurred in GMM. Under an external magnetic field, magnetization state of GMM changes and this will causes a changing of GMM rod's length. GMM rod deformation is transferred to the external load in the form of displacement through a displacement transmission mechanism. And then the external load will be driven to move.

The GMA is designed modularly and its structure is shown in Fig. 1. The driving element is a GMM rod which is made of TbDyFe. Working magnetic field is generated by a drive coil. When the drive coil is provided with current, GMM rod will elongate or shorten along the axial. Elongating distortion of GMM is transferred to the external through the upper magnetic conductive block and transmission shaft.

Magnetic flux density acting on GMM is measured by an integrated linear Hall sensor. In order to improve the magnetic field measuring sensitivity, a special structure around Hall sensor with a stainless steel ring is proposed (shonw in the amplifying part in Fig. 1(a)). It is designed according to the following principle: magnetic flux like an electric current takes the way with the least resistance. Relative magnetic permeability of stainless steel ring is near to one and it magnetically behaves like the sensor and surrounding air. Thus, magnetic flux can pass Hall sensor, stainless steel ring and air averagely.

Magnetostrictive effect characteristic of GMM is related to bias magnetic field. A method that bias current and drive current being superposed together in one drive coil is adopted to provide working magnetic field and bias magnetic field simultaneously. This driving method not only ensures adjustment convenient of bias magnetic field, but

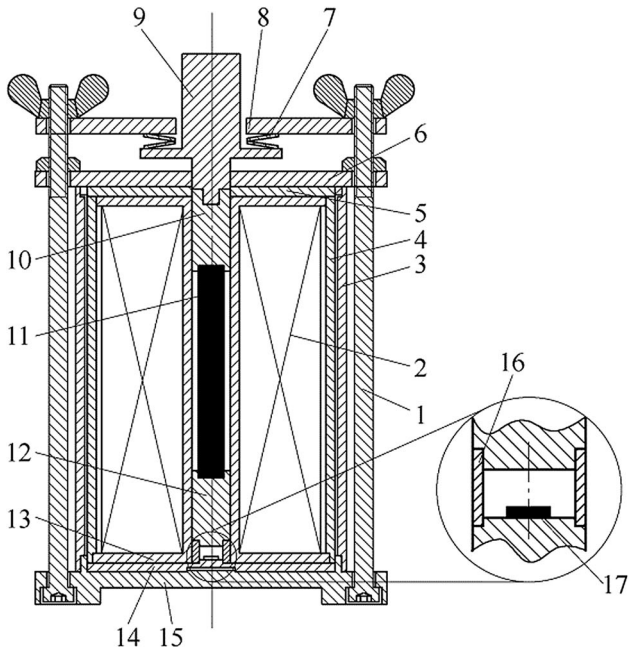

(a) 2D structure diagram

(b) Photograph of the prototype

Fig. 1 Structure of GMA 1. Preload bolts; 2. Drive coil; 3. Shell; 4. Cylindrical magnetic yoke; 5. Upper magnetic conductive cover; 6. Head cover; 7. Disc spring; 8. Preload cover; 9. Transmission shaft; 10. Upper magnetic conducti ve block; 11. GMM rod; 12. Under magnetic conductive block; 13. Drive coil frame; 14. Under magnetic conductive cover; 15. Bottom cover; 16. Stainless steel ring; 17. Hall sensor

also overcomes the massive structure problem of actuator which has double coils. Due to its quite low magnetic permeability, GMM is not suitable to be used as flux guiding element. The magnetic conductive block, magnetic conductive cover and cylindrical magnetic yoke made of highly permeable electromagnetic pure iron are designed to work as the flux guidance elements and ensure that magnetic flux density distributes uniformly in GMM.

Preload cover and disc spring constitute a preload mechanism which provides a pre-tightening force to GMM and other the internal structures. It prevents internal structures from loosening and improves GMM's magnetostrictive performance. In order to realize fine adjustment of pre-tightening force conveniently, two disk springs with involution combination mode is adopted. Pre-tightening force can be adjusted with the thread fit distance between preload bolts and their butterfly nuts.

Therefore, a GMA which can output high-precision displacement mainly consists of driving mechanism module and preload mechanism module. Driving mechanism module completes the functions of GMM driving and magnetic field measurement. It mainly includes: GMM rod, drive coil, magnetic guiding structures, measuring device of magnetic flux density, displacement transmission mechanism, shell and other external packaging structures. Preload mechanism module completes the function of providing preload to GMM. And it mainly includes preload cover, disc spring, preload bolts and butterfly nuts et al.

3 Modeling for GMA Considering the Magnetic Hysteresis and Energy Loss

3.1 Establishing of the Constitutive Relations Between Magnetization and Magnetostriction

In this section, on the basis of Armstrong theory and through analyzing the composition of GMM's internal elastic Gibbs free energy, a constitutive model which describes the magnetization process and magnetostriction process for GMM is established. In the process of model establishment, a three-dimensional anisotropic model is adopted to deeply analyze the occurrence mechanism of magnetostrictive effect for GMM. In order to simplify the modeling process to some extent, internal interaction among GMM domains is ignored in the modeling process.

Atoms column in every direction in the crystal is called crystal orientation, and it is denoted by crystal orientation index [20]. For example, a displacement vector from an atom to the nearest atom along the crystal orientation is $l_1\sigma_1 + l_2\sigma_2 + l_3\sigma_3$, in which parameters σ_1, σ_2 and σ_3 are lattice basis vectors. This crystal orientation is marked by crystal orientation index $<l_1 l_2 l_3>$. Figure 2 shows one cubic primitive cell of a simple cubic lattice. Crystal orientation of cubic edge OA is <100>. Crystal orientation of the diagonal of face OB is <110>. Crystal orientation of the body diagonal OC is <111>. Because the crystal is anisotropic, it leads to magnetic crystalline energy needed in the magnetization process along different directions are different. Therefore, there is a direction in which the magnetic crystalline energy is needed when each

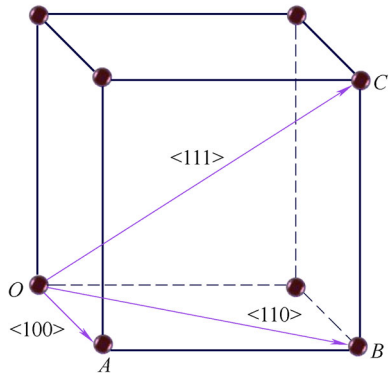

Fig. 2 Schematic diagram of cubic primitive cell in a simple cubic lattice

ferromagnet is magnetized is the minimum. This direction is called the easy magnetization direction.

When GMM is under the action of magnetic field and magnetized, the internal elastic Gibbs free energy can be written as

$$E_t = E_k + E_H + E_\sigma + E_d, \tag{1}$$

where E_t is the internal elastic gibbs free energy of GMM.E_k, E_H, E_σ and E_d are the magneto crystalline anisotropy energy, magnetic energy, stress energy and demagnetizing energy respectively in GMM. Usually, ratio between the height and width of the GMM used in GMA is larger. And high aspect ratio leads to the demagnetization effect inside the material is very weak, therefore the fourth item in the right end of Eq. (1), namely the demagnetizing energy, can be ignored in the process of modeling. In other words, the total energy within GMM is composed of magneto crystalline anisotropy energy, magnetic energy and stress energy approximately. These three kinds of energy are described by crystal orientation index, crystallographic orientation cosine and other variables.

The magneto crystalline anisotropy energy of GMM is expressed by magneto crystalline anisotropy coefficient and crystallographic orientation cosine,

$$E_k = K_1\left(\alpha_1^2\alpha_2^2 + \alpha_2^2\alpha_3^2 + \alpha_3^2\alpha_1^2\right) + K_2\alpha_1^2\alpha_2^2\alpha_3^2, \tag{2}$$

where $\alpha_i (i = 1, 2, 3)$ is the orientation cosine of magnetization with respect to crystal axis. K_1 and K_2 are magneto crystalline anisotropy coefficient. For counterfeit cubic materials, the item K_2 included in the above equation is ignored generally.

Magnetic field energy in GMM is

$$E_H = \mu_0 H M_s(\alpha_1\beta_1 + \alpha_2\beta_2 + \alpha_3\beta_3), \tag{3}$$

where H represents the magnetic field intensity acting on GMM. μ_0 is the vacuum permeability. M_s is the saturation magnetization of GMM. $\beta_i (i = 1, 2, 3)$ is the orientation cosine of magnetic field intensity with respect to crystal axis.

The stress energy of GMM is described by magnetostrictive coefficient, stress, direction cosine and other parameters as

$$\begin{aligned} E_\sigma = {} & 3/2\lambda_{100}\left(\alpha_1^2\sigma_{11} + \alpha_2^2\sigma_{22} + \alpha_3^2\sigma_{33}\right) \\ & - 3\lambda_{111}(\alpha_1\alpha_2\sigma_{12} + \alpha_2\alpha_3\sigma_{23} + \alpha_1\alpha_3\sigma_{13}), \end{aligned} \tag{4}$$

where λ_{100} and λ_{111} are saturation magnetostrictive coefficients of the <100> and <111> crystal orientation respectively. $\sigma_i (i = 1, 2, 3)$ represents the component of stress acting on GMM. Therefore, when the magnetic field intensity, stress and their directions are known, magnetic anisotropy energy E_k, magnetic field energy E_H and stress energy E_σ can be calculated by Eqs. (2) – (4). And then total internal elastic Gibbs free energy of GMM can be obtained too.

At present, in the process of studying the characteristics of GMM's magnetic hysteresis, GMM is generally regarded as an ideal ferromagnetic material. That is, movement and rotation process generated by the magnetic domain along the same direction in GMM are identical. On the basis of this assumption, it can be derived that magnetic domains in GMM will change continually to ensure the domain state occupy the direction of minimum free energy. But in fact, defects of GMM bring about a part of the magnetic domain remaining in their initial states. And then it leads to the process that magnetic domain always motions towards to the direction of possession the minimum free energy is not continuous. In order to describe the motion characteristics of magnetic domain in GMM accurately, it puts forward that using magnetic potential orientation parameter to describe the degree of difficulty or ease of magnetic domain turn to the easy magnetization direction. The magnetic potential orientation distribution is expressed by a negative exponential function, and its expression is

$$P_i^{an} = C \bullet \exp\left(-E_i^t/w\right), \tag{5}$$

where P_i^{an} is anhysteretic magnetic potential orientation parameters. C is a standardized evaluation factor related to the working magnetic field and stress. E_i^t is the total Gibbs free energy in the direction of easy magnetization <111>. w is the energy distribution parameter. The subscript i represents a concrete component direction of the crystal orientation index <111>.

In magnetization process, movement and rotation of magnetic domains in GMM will result in changes of interanl magnetization and GMM's length. Total anhysteretic magnetization in GMM can be expressed as a sum of magnetization in each easy magnetization direction:

$$M_{\mathrm{an}} = \sum_{i=1}^{8} P_i^{\mathrm{an}} M_{\mathrm{s}}(\alpha_{i1}\gamma_1 + \alpha_{i2}\gamma_2 + \alpha_{i3}\gamma_3), \tag{6}$$

where M_{an} is the total of anhysteretic magnetization, α_{ij}(-$j = 1, 2, 3$) is the direction cosine of magnetization along the i_{th} easy magnetization direction. γ_I ($i = 1, 2, 3$) is a direction cosine of the measuring direction with respect to magnetization direction.

The total magnetostriction coefficient which represents the elongation ability of GMM is expressed as the sum of magnetostrictive coefficients along each easy magnetization direction direction:

$$\lambda = \sum_{i=1}^{8} p_i^{\mathrm{an}} \{3/2\lambda_{100}(\alpha_{i1}^2\gamma_1^2 + \alpha_{i2}^2\gamma_2^2 + \alpha_{i3}^2\gamma_3^2) + 3\lambda_{111}(\alpha_{i1}\alpha_{i2}\gamma_1\gamma_2 + \alpha_{i2}\alpha_{i3}\gamma_2\gamma_3 + \alpha_{i3}\alpha_{i1}\gamma_3\gamma_1)\}, \tag{7}$$

where λ is the total magnetostrictive coefficient.

3.2 Dynamic Hysteresis Magnetization and Magnetostriction Model for GMM

For an ideal GMM, movement and roatiaon of its internal magnetic domains eventually bring aoubt significant changes in the value of magnetostriction and magnetization, and the magnetic domain change process is completely reversible. But for the current GMM that is rare earth alloy material, there are eddy current loss caused by dynamic magnetic field changes, quasi static energy consumption and other forms of energy loss in the magnetization process. These energy loss makes the magnetization process of GMM is not completely reversible. According to the law of conservation of energy, a energy balance equation in the magnetization process for GMM is established as

$$E = E_{\mathrm{sta}} + L_{\mathrm{pin}} + L_{\mathrm{e}} + L_{\mathrm{a}}, \tag{8}$$

where E is the total energy of working magnetic field per unit volume in GMM. E_{sta} is magnetic energy stored in the material. L_{pin} is the energy loss caused by hysteresis per unit volume in the pinning state. L_{e} is the energy loss caused by eddy current per unit volume. L_{a} is the abnormal energy loss per unit volume.

Total energy per unit volume of the working mangnetic field is defined as a product of vacuum permeability and the integration of anhysteretic magnetization:

$$E = \mu_0 \int M_{\mathrm{an}} \mathrm{d}H. \tag{9}$$

Magnetic energy stored in GMM is defined as a product of vacuum permeability and the integration of magnetization:

$$E_{\mathrm{sta}} = \mu_0 \int M \mathrm{d}H. \tag{10}$$

Energy loss per unit volume caused by hysteresis is expressed as a product of vacuum permeability and the integration of energy loss coefficient:

$$L_{\mathrm{pin}} = \mu_0 \int k \mathrm{d}M, \tag{11}$$

where parameter k is a quasi static energy loss coefficient and it is a constant that is greater than or equal to zero.

Energy loss per unit volume caused by the eddy current is described as

$$L_{\mathrm{e}} = \frac{\mu_0^2 D^2}{2\rho\eta} \int (\mathrm{d}M/\mathrm{d}t)^2 \mathrm{d}t, \tag{12}$$

where D represents the critical dimensions of GMM, such as thickness of GMM sheet or diameter of cylindrical GMM rod. ρ is the resistivity of GMM. η is the geometrical factor of GMM. From analyzing the above equation, it can be known that eddy currents will become larger with the increasing of frequency.

Moreover, at the same time of the alternating magnetic field generating eddy currents, GMM will have skin effect. That is to say, current dose not distribute uniformly on the cross section of GMM and the current will concentrates on the surface. The higher the frequency, the skin effect is more obvious. However, if the skin effect is considered in the process of modeling, formula processing will be very complex. Therefore, when it is calculating eddy current losses, skin effect is ignored generally. That is, when Eq. (12) is used, it is usually assumed that the distribution of magnetic field inside GMM is uniform.

Abnormal energy loss per unit volume is as follows:

$$L_{\mathrm{a}} = \mu_0^{3/2} \left(\frac{GSV_0}{\rho}\right)^{1/2} \int (\mathrm{d}M/\mathrm{d}t)^{3/2} \mathrm{d}t, \tag{13}$$

where S is the cross-sectional area of GMM; G is a dimensionless coefficient which is used to evaluate the damping effect of eddy current. V_0 expresses the magnetic domain inner potential. When GMM works under quasi static state, eddy current loss caused by dynamic magnetic field and the abnormal energy loss in the right side of energy balance Eq. (8) are deleted, and then the basic energy balance equation for GMM working in quasi static will be obtained:

$$E = E_{\mathrm{sta}} + L_{\mathrm{pin}}. \tag{14}$$

In order to express the energy balance equation and various energy dissipation expression as the relationship among energy, magnetization, magnetic field intensity, working time and other macroeconomic variables, the

above expressions are done a mathematical processing. The specific process is as follows.

In the eddy current loss Eq. (12), $(\mathrm{d}M/\mathrm{d}t)^2\mathrm{d}t$ is expressed as $(\mathrm{d}M/\mathrm{d}t)(\mathrm{d}M/\mathrm{d}H)\mathrm{d}H$, and then the equation becomes

$$\begin{aligned} L_{\mathrm{e}} &= \frac{\mu_0^2 D^2}{2\rho\eta}\int (\mathrm{d}M/\mathrm{d}t)^2\mathrm{d}t \\ &= \frac{\mu_0^2 D^2}{2\rho\eta}\int (\mathrm{d}M/\mathrm{d}t)(\mathrm{d}M/\mathrm{d}H)\mathrm{d}H. \end{aligned} \tag{15}$$

In the abnormal energy loss Eq. (13), the item $(\mathrm{d}M/\mathrm{d}t)^{\frac{3}{2}}\mathrm{d}t$ is modified as $(\mathrm{d}M/\mathrm{d}t)^{1/2}(\mathrm{d}M/\mathrm{d}H)\mathrm{d}H$, and then this equaion is expressed as

$$\begin{aligned} L_{\mathrm{a}} &= \mu_0^{3/2}(GSV_0/\rho)^{1/2}\int (\mathrm{d}M/\mathrm{d}t)^{3/2}\mathrm{d}t \\ &= \mu_0^{3/2}(GSV_0/\rho)^{1/2}\int (\mathrm{d}M/\mathrm{d}t)^{1/2}(\mathrm{d}M/\mathrm{d}H)\mathrm{d}H. \end{aligned} \tag{16}$$

Equations (9) –(11), (15) and (16) are substituted into Eq. (8), a mathematical relationship among anhysteretic magnetization, magnetization, magnetic field intensity and time for GMM is obtained:

$$\begin{aligned} \mu_0\int M_{\mathrm{an}}\mathrm{d}H &= \mu_0\int M\mathrm{d}H + \mu_0 k\int \mathrm{d}M/\mathrm{d}H\mathrm{d}H \\ &+ \mu_0^2\frac{D^2}{2\rho\eta}\int (\mathrm{d}M/\mathrm{d}t)(\mathrm{d}M/\mathrm{d}H)\mathrm{d}H + \\ &\mu_0^{3/2}(GSV_0/\rho)^{1/2}\int (\mathrm{d}M/\mathrm{d}t)^{1/2}(\mathrm{d}M/\mathrm{d}H)\mathrm{d}H. \end{aligned} \tag{17}$$

The two ends of Eq. (17) are taked H derivation, and then are devided by μ_0. Thus, the integral terms in Eq. (17) will be eliminated and the equation is changed into

$$\begin{aligned} M_{\mathrm{an}} &= M + k\mathrm{d}M/\mathrm{d}H + \mu_0\frac{D^2}{2\rho\eta}(\mathrm{d}M/\mathrm{d}t)(\mathrm{d}M/\mathrm{d}H) \\ &+ \mu_0^{1/2}\left(\frac{GSV_0}{\rho}\right)^{1/2}(\mathrm{d}M/\mathrm{d}t)^{1/2}(\mathrm{d}M/\mathrm{d}H). \end{aligned} \tag{18}$$

In a easy magnetization direction of GMM, relationship among the change of magnetization, saturation magnetization and magnetic potential orientation parameter in this direction is

$$\mathrm{d}M_i = M_{\mathrm{s}}\mathrm{d}p_i. \tag{19}$$

In order to be convenient to simplify mathematical model, every specific component of crystal orientation <111> is manipulated seperately.

The relationship between variation of magnetization and magnetic potential orientation parameter shown in Eq. (19) is substituted into Eq. (18), and then the Eq. (18) is becomes after mathematical processing

$$\begin{aligned} P_i^{\mathrm{an}} &= P_i + k\mathrm{d}P_i/\mathrm{d}H + M_{\mathrm{s}}\mu_0 D^2/2\rho\eta(\mathrm{d}P_i/\mathrm{d}H)^2\mathrm{d}H/\mathrm{d}t \\ &+ M_{\mathrm{s}}^{1/2}(\mu_0 GSV_0/\rho)^{1/2}(\mathrm{d}P_i/\mathrm{d}H)^{3/2}(\mathrm{d}H/\mathrm{d}t)^{1/2}. \end{aligned} \tag{20}$$

where the i_{th} component of anhysteretic magnetic potential orientation parameter P_i^{an} of magnetic domain in the crystal orientation <111> can be calculated by Eq. (5). According to Eq. (20), it knows that eddy current energy loss caused by the change of dynamic magnetic field is proportional to the rate of magnetic field change versus time; While, abnormal energy loss is proportional to the square root of the rate of magnetic field change versus time. For the GMA designed in this paper, when its drive coil is provided a sinusoidal AC working current with a fixed frequency, the generated working magnetic field is a sinusoidal AC magnetic field which has a same frequency with the working current. At this time, the eddy current energy loss will be proportional to the working frequency of GMA, and the abnormal energy loss will be proportional to the square root of the working frequency.

Equation (20) is a differential equation which contains items of $\mathrm{d}P_i/\mathrm{d}H$, $(\mathrm{d}P_i/\mathrm{d}H)^2$, $(\mathrm{d}P_i/\mathrm{d}H)^{3/2}$ and $(\mathrm{d}H/\mathrm{d}t)^{1/2}$, therefore it is difficult to solve the analytical solution of magnetic potential orientation parameter P_{i} through conventional mathematical methods. Thus, in this section, it puts forward a solution method that the above differential equation is discretized using the Euler method firstly, and then the discretization equation is solved by a numerical analysis method. Equation (20) is discretized and the obtained discretization equation is as follows:

$$\begin{aligned} &\frac{(\mu_0 GSV_0 M_s)^{1/2}}{\rho^{1/2}\Delta H\Delta t^{1/2}}\left(P_i^{(j+1)} - P_i^{(j)}\right)^{3/2} + \frac{k}{\Delta H}\left(P_i^{(j+1)} - P_i^{(j)}\right) \\ &+ \frac{D^2\mu_0 M_{\mathrm{s}}}{2\rho\eta\Delta H\Delta t}\left(P_i^{(j+1)} - P_i^{(j)}\right)^2 + P_i^{(j)} - P_i^{(j)\mathrm{an}} = 0, \end{aligned} \tag{21}$$

where subscript j represents the iteration number.

Therefore, when it knows the initial value of magnetic field $H^{(0)}$ applied on GMM and the i_{th} component of magnetic potential orientation parameter $P_i^{(0)}$ in crystal orientation <111>, nonlinear Eq. (21) can be numerically solved by Newton - Ralph monson method through setting reasonable magnetic field intensity increment ΔH and time increment Δt. And then, magnetic potential orientation parameter P_i. will be calculated. The calculated anhysteretic magnetic potential orientation parameter P_i^{an} is substitued into the total anhysteretic magnetization Eq. (6) and the total magnetostrictive coefficient Eq. (7), the anhysteretic magnetization M_{an} in GMM and total magnetostrictive coefficient λ can be determined. Based on the calculated magnetic potential orientation parameters P_i,

total magnetization in GMM is obtained. Therefore, Eqs. (1)– (19) are the nonlinear magnetiztion and magnetostriction model established in this paper which includes the hysteresis characteristics and energy loss characteristic of GMM.

3.3 Kinematics Model for GMA

According to the structure of GMA, when ma According to the structure of GMA, when magnetostrictive effect occurs, the magnetostrictive displacement of GMM rod is transmitted to the outer load through upper magnetic conductive block, transmission shaft and other transmission components. In the displacement transmission process, due to the existence of a mechanical system load, magnetostrictive displacement of GMM rod is not the actual displacement outputted of GMA. The actual output displacement or force of GMA depends mainly on the deforming length of GMM rod. But, at the same time these are also affected by the displacement transmission and output mechanism of GMA. Therefore, in order to describe the actual displacement of GMA accurately, it needs to build a kinematics model of mechanical system for GMA. In the process of kinematics model establishment, the transmission shaft, upper magnetic conductive block, upper magnetic conductive gasket and head cover are regarded as ideal rigid body. Disc springs have stiffness and damping. GMM rod is a mass spring damping system with a single degree of freedom, and its lower end displacement is zero when it is moving.

3.3.1 Static Load

The simplified mechanical system model for GMA is shown in Fig. 3. Using the Newton law and D'Alembert's theory, GMM, output mechanism and shell are done force analysis and their differential equation models are established respectively.

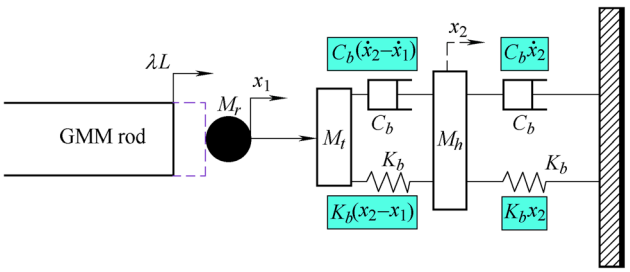

Fig. 3 Equivalent mechanical model of GMA

$$\begin{cases} \Delta\sigma_o A_r = M_r\ddot{x}_1 + C_r\dot{x}_1 + K_r x_1 - EA_r\lambda, \\ \Delta\sigma_o A_r = -M_t\ddot{x}_1 - C_b(\dot{x}_1 - \dot{x}_2) - K_b(x_1 - x_2), \\ M_h\ddot{x}_2 = -K_b(x_2 - x_1) - C_b(\dot{x}_2 - \dot{x}_1) - K_h x_2 - C_h\dot{x}_2, \\ EA_r = K_r L, \end{cases} \tag{22}$$

where x_1 is the load displacement. x_2 is a intermediate displacement variable which is set to eliminate the load effect. $\Delta\sigma_o$ is output stress of the GMM rod. M_r is the equivalent mass of GMM rod, M_t is the mass sum of load and transmission shaft, M_h is the mass sum of shell and coil. L is the initial length of GMM rod. C_r is the equivalent damping coefficient of GMM rod, C_b is the equivalent damping coefficient of disc spring. K_r is the equivalent stiffness of GMM rod, K_b is the equivalent stiffness of disc spring. A_r is the cross area of GMM rod.

Each expression of Eq. (22) is done a Laplace transformation, and the transfer function $G(s)$ between output displacement of GMA and magnetostrictive deformation of GMM rod is deduced,

$$G(s) = \frac{x_1(s)}{L\lambda(s)} = \frac{K_r}{(M_r + M_t)s^2 + (C_r + C_b)s + K_r + K_b - \frac{(C_b s + K_b)^2}{M_h s^2 + 2C_b s + 2K_b}}. \tag{23}$$

In the quasi-static condition, influence of s^2 and s on the output characteristics of the whole system are very small, therefore they are ignored in the process of researching the dynamics model for GMA. After a simplification of the above equation, a mathematical relationship in the complex domain between GMA's output displacement and magnetostriction coefficient under quasi-static conditions is obtained:

$$x_1(s) = \frac{LK_r\lambda(s)}{K_r + K_b/2}. \tag{24}$$

Equation (24) is done an inverse Laplace transformation, and the mathematical relationship in the time domain between GMA's output displacement and magnetostriction coefficient is obtained:

$$x_1 = L^{-1}\left[\frac{LK_r\lambda(s)}{K_r + K_b/2}\right] = \frac{LK_r}{K_r + K_b/2}\lambda. \tag{25}$$

The magnetostrictive coefficient λ which is calculated by Eqs. (1)–(19) is substituted into the above equation. And then, output displacement of GMA will be obtained.

3.3.2 Dynamic Load

When the output end of GMA is connected with a dynamic load, stable output force of the actuator will be influenced by the external system. Taking the GMA which is connected with an elastic load as the research object, that is,

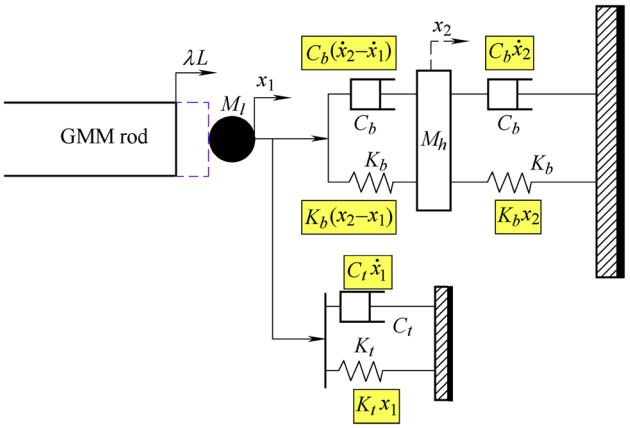

Fig. 4 Equivalent mechanical model of GMA connecting a dynamic load

the GMA being under the action of a dynamic load, the mechanical system of GMA is simplified. And the equivalent mechanical model is obtained and it is shown in Fig. 4.

Using the Newton law and D'Alembert's theory, GMM, output mechanism and shell are done force analysis and their differential equation models are established respectively:

$$\begin{cases} \Delta\sigma_o A_r = M_r\ddot{x}_1 + C_r\dot{x}_1 + K_r x_1 - EA_r\lambda, \\ \Delta\sigma_o A_r = -M_l\ddot{x}_1 - C_b(\dot{x}_1 - \dot{x}_2) - K_b(x_1 - x_2) - C_t\dot{x}_1 - K_t x_1, \\ M_h\ddot{x}_2 = -K_b(x_2 - x_1) - C_b(\dot{x}_2 - \dot{x}_1) - K_b x_2 - C_b\dot{x}_2, \\ EA_r = K_r L. \end{cases} \tag{26}$$

where C_t is the equivalent damping coefficient of elastic load. K_t is the equivalent stiffness of elastic load.

The above equation is done a Laplace transformation, and output displacement of GMA in the complex domain is deduced:

$$x_1(s) = \frac{K_r L\lambda(s)}{(M_r + M_l)s^2 + (C_r + C_b + C_l)s + K_r + K_b + K_t - \frac{(C_b s + K_b)^2}{M_h s^2 + 2C_b s + 2K_b}}. \tag{27}$$

In the complex domain, output force of GMA is

$$F(s) = \left[M_l s^2 + (C_t + C_b)s + (K_t + K_b)\right]x_1(s). \tag{28}$$

Pressure of the load in complex domain is

$$F_t(s) = (C_t s + K_t)x_1(s). \tag{29}$$

In the quasi-static condition, items of s^2 and s are ignored, and the output displacement of GMA and force of load are

$$x_1(s) \approx \frac{K_r L\lambda(s)}{K_r + K_t + K_b/2}, \tag{30}$$

$$F_t(s) \approx K_t \frac{K_r L\lambda(s)}{K_r + K_t + K_b/2}. \tag{31}$$

Equations (30)–(31) are done inverse Laplace transformation, and the mathematical relationship of GMA's output displacement and force of load in the time domain are as follows respectively

$$x_1 \approx \frac{K_r L}{K_r + K_t + K_b/2}\lambda, \tag{32}$$

$$F_t \approx \frac{K_t K_r L}{K_r + K_t + K_b/2}\lambda. \tag{33}$$

The magnetostrictive coefficient λ which is calculated by Eqs. (1)–(19) is substituted into Eq. (32) and Eq. (33). And then, the output displacement and force of GMA will be obtained.

4 Experiments and Discussion

In order to analyze the magnetization characteristic, magnetostriction, magnetic potential orientation, energy loss characteristic and other working performances for GMM, based on the nonlinear dynamic hysteresis magnetization model established in the previous section and shown as Eqs. (1)–(19), the characteristics of GMM under different magnetic field are calculated and simulated. And, the key characteristics are analyzed and discussed. Moreover, using the kinematics model of mechanical system for GMA, the mathematical relationships among GMA's output displacement and output force, GMM's elongation and system stiffness are analyzed. A set of experiments are carried out to verify the established model for GMA which considers the hysteresis and energy loss. And dynamic characteristic of GMA is analyzed.

In the process of simulating and calualting magnetization characteristic, magnetostriction, magnetic potential orientation and energy loss characteristic for GMM, the mainly used parameters are shown in Table 1. These parameters' value are determined by the genetic and simulated annealing identification algorithm which was proposed by the authors earlier [21].

GMM used in the GMA involved in this paper is a positive magnetostrictive material TBDyFe which is developed by China south rare earth functional materials research institute. It is a cylindrical rod material which diameter and length are 8 mm and 67 mm respectively. The drive coil has 1775 turns.

The experimental system for measuring GMM's magnetostriction and GMA's output displacement is shown in Fig. 5. The power supply selected in the experimental system is a high speed bipolar programmable power (BP4610) which output accuracy is ±0.001A.

Table 1 Main feature parameters of GMM

Parameters	λ_{100}	$M_s/(\mathrm{A \bullet m^{-1}})$	λ_{111}	η	$k/(\mathrm{A \bullet m^{-1}})$
Values	82×10^{-6}	6.2×10^{5}	1358×10^{-6}	14.2	8697
Parameters	G	$V_0/(\mathrm{A \bullet m^{-1}})$	$K_1/(\mathrm{J \bullet m^{-3}})$	$\rho/(\Omega \bullet \mathrm{m^{-1}})$	$w/(\mathrm{J \bullet m^{-3}})$
Values	0.169	12.6	-5.9×10^{4}	2.9×10^{-6}	11 030

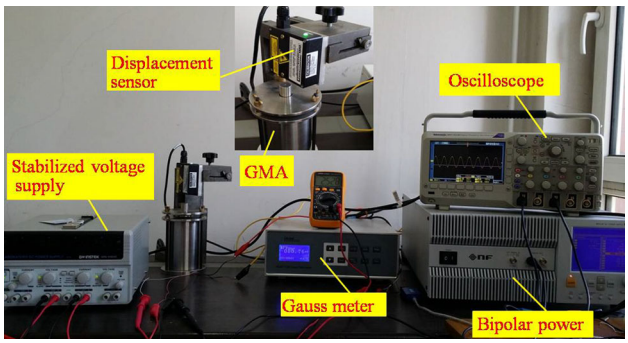

Fig. 5 Photograph of GMA experiment system

Programmable power BP4610 can supply AC drive current and DC bias current to GMA at the same time. A laser displacement sensor is used to measure the output displacement produced by GMA. Magnetostrictive coefficients are directly measured by 2×3 group of high sensitivity strain gauges which are uniformly distributed on GMM rod. Namely, three strain gauges are uniformly distributed along the axial direction and two strain gauges are uniformly distributed along the radial direction. Gauss meter CH-1500 is used to directly measure the actual magnetic field generated by driving coil under the action of current. Magnetization is measured by a Hall sensor with high sensitivity which is integrated on the bottom of GMM rod. Output signal of strain gauges bridge circuit and the laser displacement sensor are collected and monitored by a fluorescence oscilloscope. The initial magnetization state in GMM rod is adjusted repeatedly by the coordination of BP4610 power and a Hall sensor integrated in the actuator so as to make GMM rod being in the no remanence sate.

4.1 Validation of the Magnetization and Magnetostriction Model

In order to verify that the established model which is used to describe the hysteresis characteristics and magnetostrictive properties of GMM in the GMA, simulation calculation values of magnetization and magnetostriction coefficient are compared with the measured result respectively. In the experiment, the high speed bipolar power supply provides GMA with AC sinusoidal current. And it makes amplitude of the driving magnetic field is in the range of –20KA/m ~ 20kA/m, frequencies are 100 Hz and 1000 Hz respectively, and the phase of driving magnetic field is zero. Actual magnetic field of the driving coil intensity is directly measured by the Gauss meter. Based on the proportion relation between the magnetization at the bottom surface of GMM rod and the average magnetization in GMM rod which is analyzed through finite element method [22], magnetization value measured by Hall sensor is converted into the effective magnetization value of GMM rod. Theoretical values calculated by the above

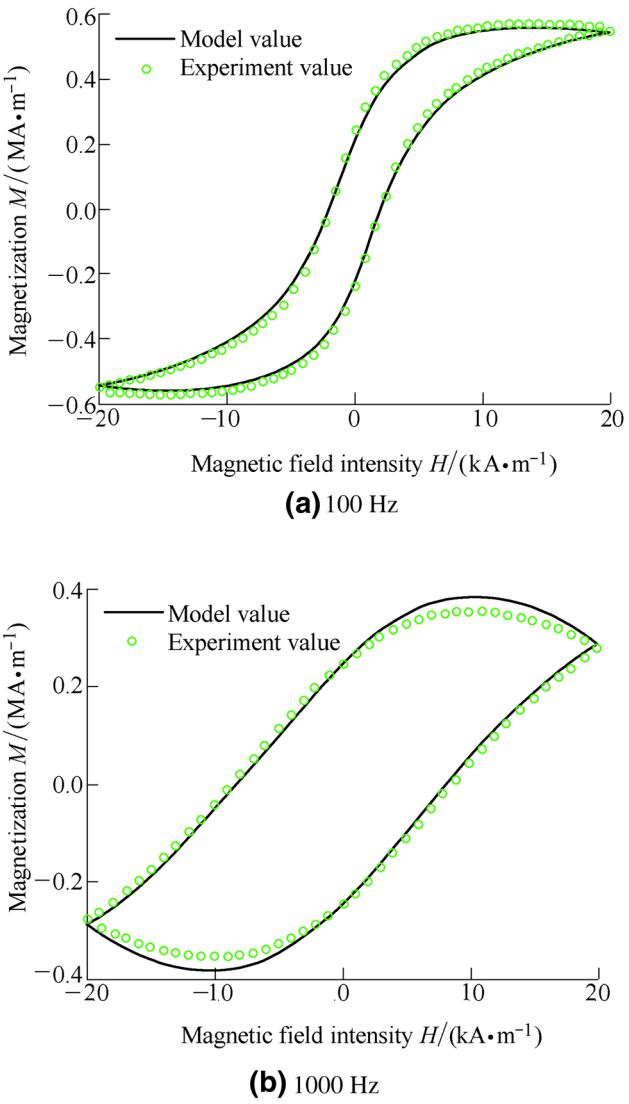

Fig. 6 Comparison diagram between calculated value and measured value of magnetization

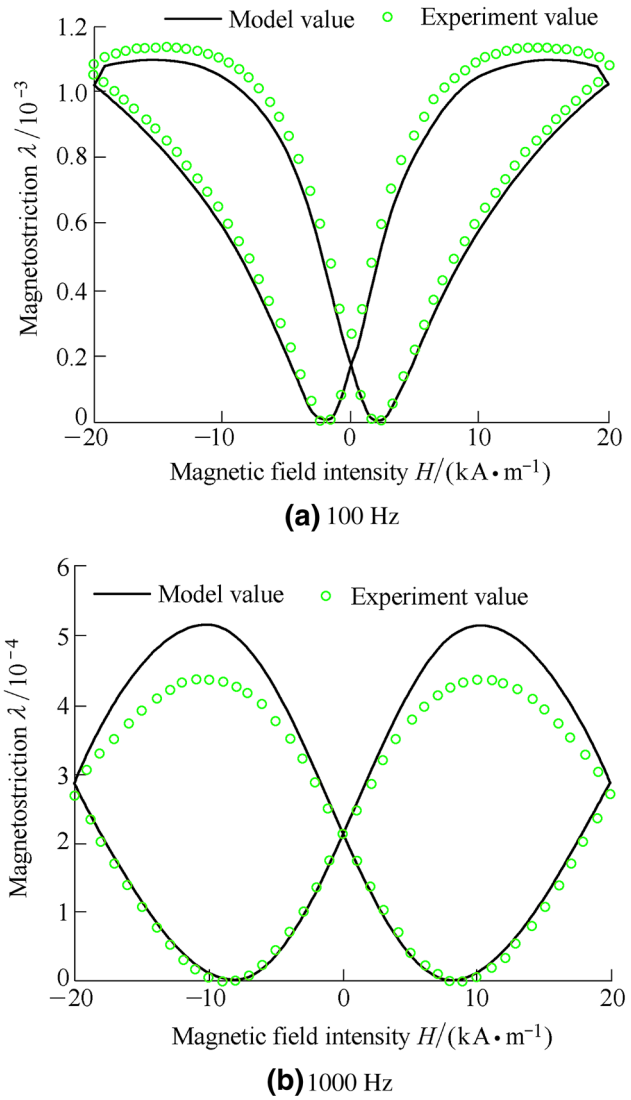

Fig. 7 Comparison diagram between calculated value and measured value of magnetostriction coefficient

model and experimental measuring values of the magnetization and magnetostriction coefficient at frequencies of 100 Hz and 1000 Hz are shown in Fig. 6 and Fig. 7. Result shows that there are hysteresis for magnetization and magnetostriction coefficient of GMM. Moreover, with the increasing of frequency, hysteresis becomes larger. It is caused by the increasing of energy loss. According to the J-A magnetic theory, total magnetization in GMM is composed of reversible magnetization and irreversible magnetization. Irreversible magnetization is caused by the energy consumption of irreversible domain in the process of movement, and it manifests as hysteresis characteristic of GMM at macro level.

Theoretical result of magnetization and magnetostriction coefficient calculated by the model are in good agreement with experimental values in general. There are some deviations between the two near –5KA/and 15KA/m in the return process. And the deviation is mainly attributed to the following two aspects: On the one hand, to simplify the modeling process, the established magnetization model does not consider the impact extent of reversible magnetization process and irreversible magnetization process on the total magnetization results in this paper. On the other hand, in the modeling process, magnetization process is confined to the easy magnetization direction, and rotating process of magnetic domains in the other crystal orientation to the easy magnetization direction is ignored. Thus, the theoretical value of magnetization and magnetostriction are slightly smaller than the experimental value.

4.2 Magnetic Domain Distribution and its Influence on Magnetostrictive Property

When GMA works in the magnetic field which frequency is 500 Hz and amplitude is in the range of –20 KA/m ~ 20 KA/m, magnetostrictive coefficient of GMM in <110>, <111> and <112 > crystal orientation are computed respectively. Magnetostrictive curves in different crystal orientation are obtained and are shown in Fig. 8. The results show that magnetostrictive coefficient of <111> crystal orientation is much larger than that of <110> and <112> crystal orientation. This shows that the strain caused by magnetic field in the <111> crystal orientation is generated by the process that magnetic domain rotates from a completely free distribution state to the <111> crystal orientation. In other words, the strain caused by magnetic field in the <111> easy magnetization direction is larger than that of <112> and <110> easy magnetization direction. According to the above conclusion, under the same magnetic field, GMM whose easy magnetization direction

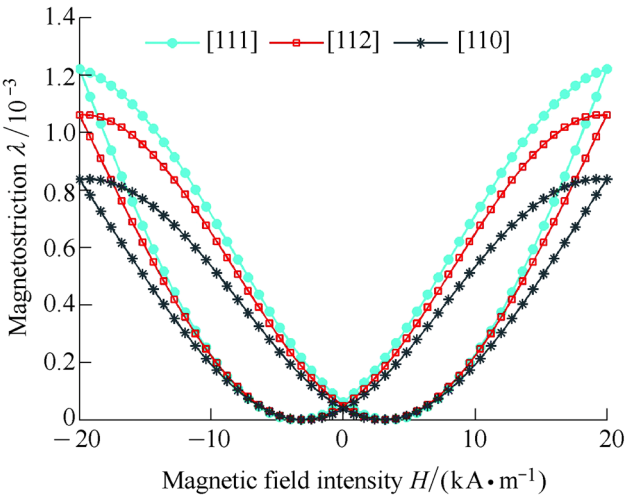

Fig. 8 Calculated result of magnetostriction in different crystal orientation

toward <111> crystal orientation has a larger magnetostriction ability. Therefore, GMM rod which easy magnetization direction toward <111> crystal orientation is more suitable to using as the driving material for GMA.

In order to analyze the impact extent of magnetic domains rotation of each crystal orientation on the total magnetization and magnetostriction characteristics of GMM, values of magnetic potential orientation, magnetization and magnetostrictive coefficient in $<\bar{1}\bar{1}1>$, $<\bar{1}\bar{1}\bar{1}>$, $<111>$, $<11\bar{1}>$, $<1\bar{1}1>$, $<1\bar{1}\bar{1}>$, $<\bar{1}11>$ and $<\bar{1}1\bar{1}>$ crystal orientation are calculated and analyzed respectively. The results are shown in Fig. 9. Figure 9(a) describes the calculated value of magnetic potential orientation of $<\bar{1}\bar{1}1>$, $<\bar{1}\bar{1}\bar{1}>$, $<111>$, $<11\bar{1}>$, $<1\bar{1}1>$, $<1\bar{1}\bar{1}>$, $<\bar{1}11>$ and $<\bar{1}1\bar{1}>$ crystal orientation of GMM. When magnetic field is less than the coercive field, magnetic potential orientation parameter value of $<\bar{1}\bar{1}1>$ and $<\bar{1}\bar{1}\bar{1}>$ crystal orientation are far greater than that of the other six crystal orientation; And when magnetic field is greater than the coercive field, magnetic potential orientation parameter value of $<111>$ and $<11\bar{1}>$ crystal orientation are far greater than that of the other six crystal orientation. Only when the magnetic field is in the vicinity of coercive field, the magnetic potential orientation parameter values of $<1\bar{1}1>$, $<1\bar{1}\bar{1}>$, $<\bar{1}1\bar{1}>$ and $<\bar{1}11>$ crystal orientation are about to be close to that of $<\bar{1}\bar{1}1>$, $<\bar{1}\bar{1}\bar{1}>$, $<111>$ and $<11\bar{1}>$.

From the result shown in Fig. 9(b), it can be known that magnetization of $<\bar{1}\bar{1}1>$ crystal orientation is equal to that of $<\bar{1}\bar{1}\bar{1}>$ crystal orientation, while magnetization of $<111>$ crystal orientation is equal to that of $<11\bar{1}>$ crystal orientation. When magnetic field is less than the coercive field, the total magnetization of GMM is approximately equal to the sum of magnetization of $<\bar{1}\bar{1}1>$ crystal orientation and $<\bar{1}\bar{1}\bar{1}>$ crystal orientation. When magnetic field is greater than the coercive field, the total magnetization is approximately equal to the sum of magnetization of $<111>$ crystal orientation and $<11\bar{1}>$ crystal orientation. While, magnetization of $<1\bar{1}1>$, $<1\bar{1}\bar{1}>$, $<\bar{1}11>$ and $<\bar{1}1\bar{1}>$ crystal orientation is almost zero. Thus, magnetic domains in $<\bar{1}\bar{1}1>$, $<\bar{1}\bar{1}\bar{1}>$, $<111>$ and $<11\bar{1}>$ direction play a leading role in the total magnetization of GMM shown in the macro level. This conclusion is the same as the analysis results for magnetic potential orientation parameter values in all the eight crystal orientation shown in Fig. 9(a). This manifests that the influence extent of magnetization in magneto crystalline direction on the total magnetization of GMM mainly depends on the magnetic potential orientation parameter value.

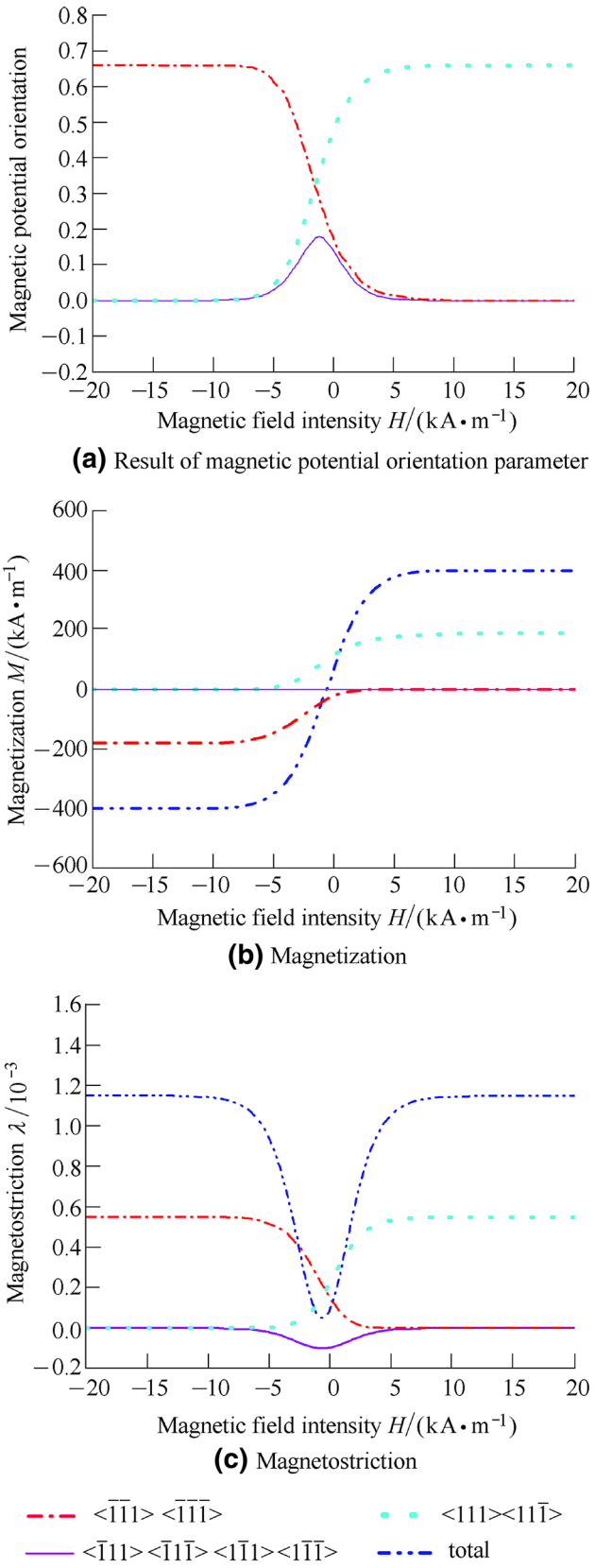

Fig. 9 Magnetization and magnetostrictive features in various crystal orientation

In addition, from the magnetostrictive coefficient curves of various crystal orientation shown in Fig. 9(c), it can be seen that when magnetic field is in the vicinity of coercive field, magnetostrictive effect in $<1\bar{1}1>$, $<1\bar{1}\bar{1}>$, $<\bar{1}11>$ and $<\bar{1}1\bar{1}>$ crystal orientation are negative and weaken the total magnetostriction performance of GMM. The total magnetization is usually able to return to its initial value in the coercive field. However, magnetostriction cannot return to its initial value. This is because that parts of magnetic domain cannot rotate back to the original distribution state in the process of magnetostrictive effect occurs, and energy loss affects the distribution of domain. And then, this leads to there is residual magnetostriction near the coercive field.

4.3 Energy Loss and its Relationship with Frequency

In order to study the composition of energy loss in GMM and the influence law of frequency on energy loss, various kinds of energy loss value in GMM are calculated while working frequency increases from 0 Hz to 4000 Hz. And the result is shown in Fig. 10. Results show that the static energy loss remains at 9.5 kJ/m^3 in general, which manifests that the static energy loss is independent on the operating frequency of GMM. Eddy current loss increases linearly with the increasing of frequency approximately. When frequency nearly increases to 1600 Hz, the eddy current energy loss is almost the same as static energy loss and its value is almost 9.5 kJ/m^3. Then, with the increasing of frequency, eddy current energy loss gradually plays a leading role in the total energy loss. With the increasing of frequency, abnormal energy loss gradually increases and there is a nonlinear relationship between them. Abnormal energy loss is much smaller than eddy current energy loss and static energy loss. And its maximum value is about 2 kJ/m^3. This shows that the abnormal energy loss behavior which occurs surrounding the domain wall is not significant in this frequency range. Therefore, abnormal energy loss is usually ignored when it calculates the magnetization and magnetostriction characteristics of GMM. But, in order to accurately express the dynamic hysteresis behavior of GMM, abnormal energy loss cannot be ignored when the static energy loss is fairly small or excitation high frequency is very high.

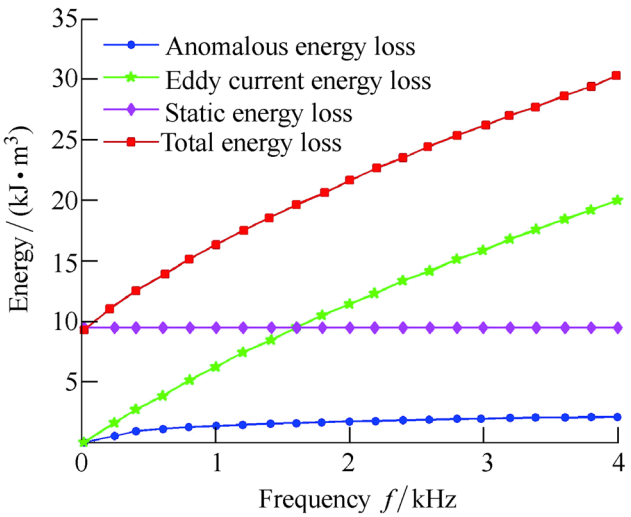

Fig. 10 Calculating result of energy loss for GMM

4.4 Analysis for the Influence Law of Frequency on Magnetization and Magnetostriction

In order to study the influence law of frequency on magnetization and magnetostriction characteristics for GMM, magnetization and magnetostriction are calculated when

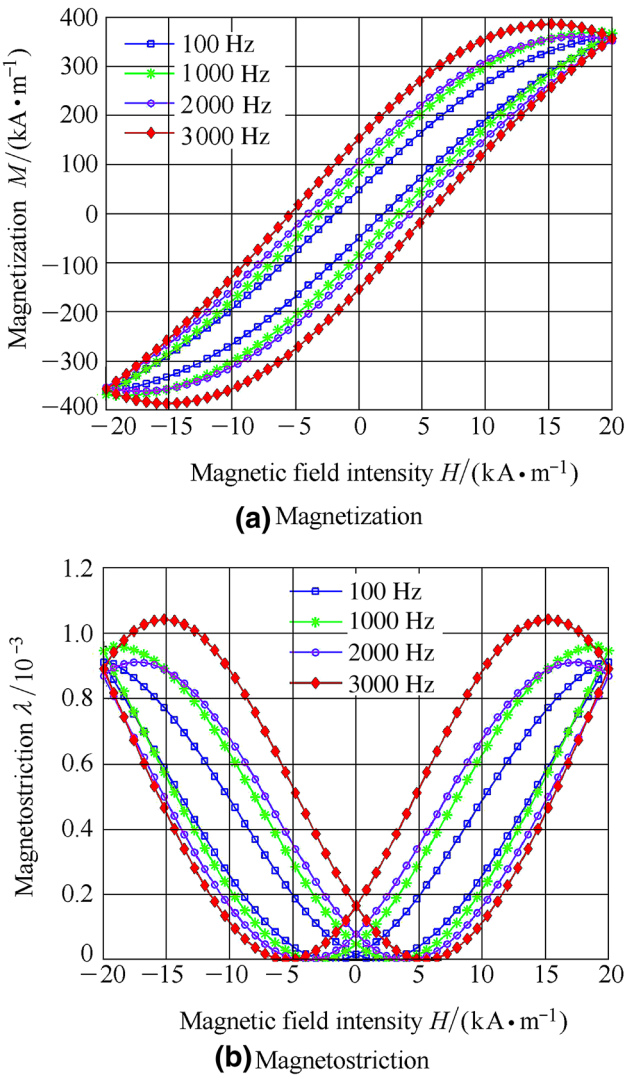

Fig. 11 Analysis results of the influence of frequency on magnetization and magnetostriction

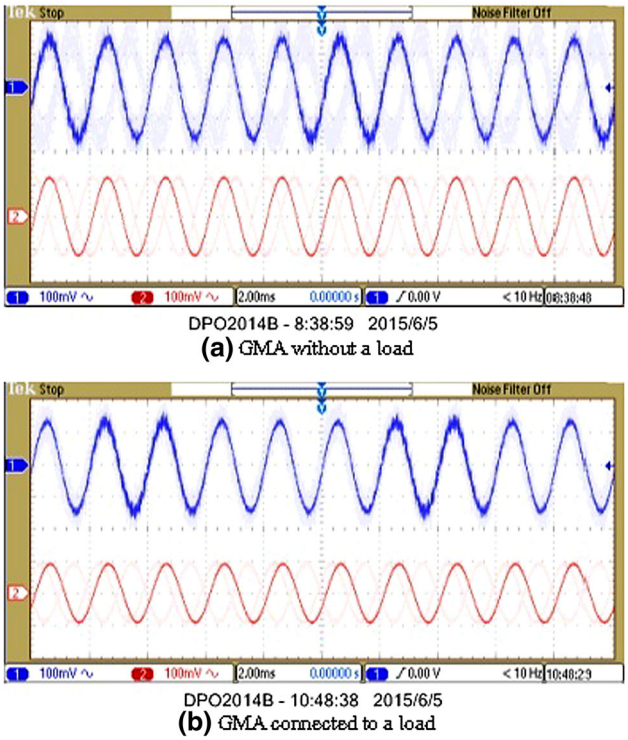

Fig. 12 Measuring result of GMM rod's elongation and GMA's output displacement (1th channel is elongation, 2nd channel is displacement)

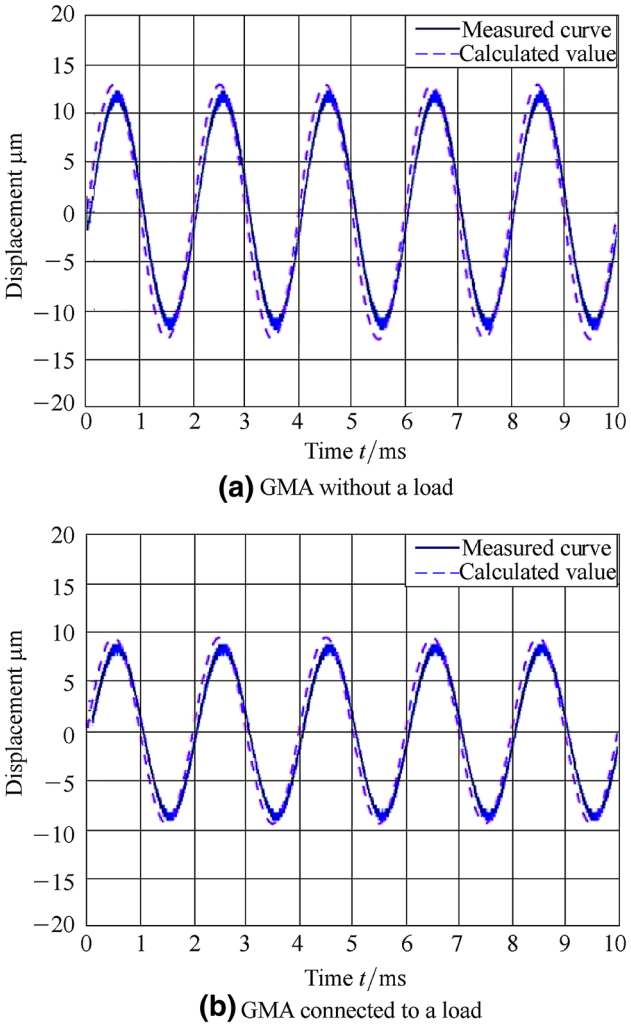

Fig. 13 Comparison between measured and theoretical result of displacement

the operating frequency of GMM are 100 Hz, 1000 Hz, 2000 Hz and 3000 Hz in this paper. The obtained magnetization and magnetostriction results for different frequency are shown in Fig. 11. From the results it can be seen that hysteresis is greater with the increase of excitation frequency; And with the increasing of frequency, residual magnetostriction is greater at the coercive field. This is because that the eddy current loss and abnormal loss increase with the increasing of frequency. And this leads to a gradual increasing of the total energy loss and the number of magnetic domain which cannot be return back to the initial state distribution. These issues are manifested as that with the increasing of frequency, hysteresis value on magnetization curve and magnetostriction curve gradually increases and the residual magnetostriction is greater in the macro level.

4.5 Analysis of the kinetic characteristic for GMA

Based on the above established hysteresis magnetostriction model of GMM and the kinematics model of GMA mechanical systems, elongation of GMM rod and output displacement of GMA are calculated respectively. Equivalent stiffness of GMM rod K_r, equivalent stiffness of disc spring K_b are determined as 9.2 MN/m and 5.9 MN/m respectively through the finite element mechanical characteristics analysis method. At the same time, the high speed bipolar programmable power supplies GMA with AC current and the GMA is experimented and tested. Elongation of GMM rod is measured through the 2×3 groups of high sensitive resistance strain gauge pasted on GMM rod. Output displacement of GMA is measured by the laser displacement sensor. Meanwhile, output signals of the strain gauge bridge and laser displacement sensor are monitored and saved by the fluorescence oscilloscope in real time.

When GMA works under the driving current which frequency is 500 Hz and amplitude is 1.5 A, the calculated value and experimental results of GMM rod's elongation and GMA's output displacement are shown in Fig. 12 and Fig. 13. Results show that when there is no load connected to GMA, ratio between the elongation of GMM rod and the output displacement of GMA is nearly 1.35. When stiffness of the load connected to GMA is $K_t = 1.9$ MN/m, GMA's

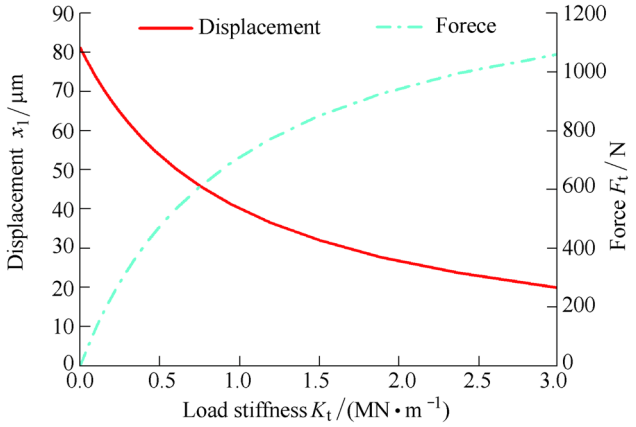

Fig. 14 Relation curves between output displacement or force and load stiffness

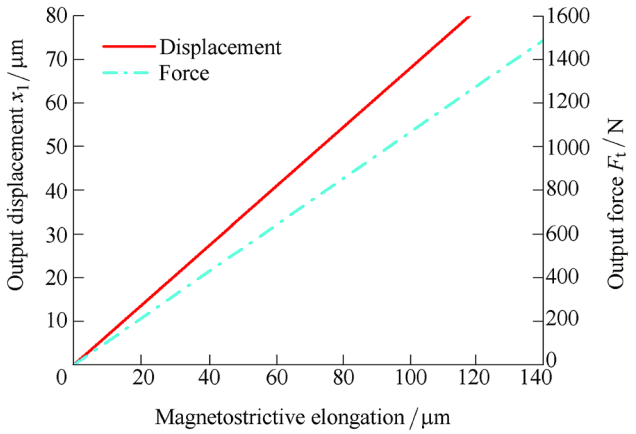

Fig. 15 Relationship between output displacement or force and magnetostrictive displacement

output displacement is almost 0.67 times of the GMM rod's elongation. While GMA is without a load or connected a load, there is a little deviation between the theoretical value and measured value of output displacement. Average relative errors are 3.8% and 4.5% respectively. It can get the following conclusion that the kinematic model of GMA established in this paper is able to accurately describe the relationship between GMM's elongation and GMA' output displacement and other kinematic characteristics in general.

In order to clear the relationship between output displacement and force of GMA and load stiffness, the output displacement and output force of GMA are calculated while the equivalent stiffness K_t of elastic load changes from 0 to 3 MN/m. In this simulation process, GMA is under a quasi static working condition. And the results are shown in Fig. 14. According to the relationship curves between elastic load stiffness and output displacement and output force of the actuator, output displacement decreases with the increase of stiffness. And the displacement will reach to 0 at last. While, the output force will gradually increase until reaching to a saturation state. The saturation output force is directly related to the stiffness of GMM.

In addition, the simulation conditions are determined as that the equivalent stiffness of GMM rod K_r, equivalent stiffness of disc spring K_b and equivalent stiffness of elastic load K_t are 9.2 MN/m, 5.9 MN/m and 1.9 MN/m approximately. While magnetostrictive displacement increases from 0 to 140μm, change process of the actual output displacement and output force has been calculated for GMA. Relationship curves among the actuator's displacement or force and magnetostrictive displacement are shown in Fig. 15. It can be seen that, when the elastic load stiffness keeps constant, there is a linear relationship between output displacement or force of the actuator and magnetostrictive displacement.

5 Conclusions

(1) A new magnetostrictive and kinematic model considering the dynamic hysteresis and energy loss is established for GMA on the bsis of Armstrong theory and elastic Gibbs free energy theory. This model can be used to describe the magnetization property, magnetostriction, magnetic potential orientation, energy loss characteristic, magnetostrictive elongation and output displacement for GMA well.

(2) As frequency increases, eddy current power loss and abnormal loss gradually play a leading role in total energy loss. Energy loss affects the distribution of domain, and the number of magnetic domains which cannot return to the initial distribution state is more with the increasing of frequency in the process of GMM's magnetostrictive effect occurs. These lead to the more serious hysteresis of magnetization and magnetostriction coefficient.

(3) Moreover, the magnetostriction cannot return to its initial value in the vicinity of coercive field, namely there is residual magnetostriction.

(4) When the elastic load stiffness keeps constant, there is a linear relationship between output displacement or force of the actuator and magnetostrictive displacement.

References

1. ZHENG Jigui, HUANG Yuping, WU Hongxing, et al. Design of a transverse-flux permanent-magnet linear generator and controller for use with a free-piston stirling engine[J]. *Chinese Journal of Mechanical Engineering*, 2016, 29(4): 832–842.

2. ZHANG Zhonghua, KAN Junwu, WANG Shuyun, et al. Effects of driving mode on the performance of multiple-chamber piezoelectric pumps with multiple actuators[J]. *Chinese Journal of Mechanical Engineering*, 2015, 28(5): 954–963.
3. NAKANO H. Angstrom positioning system using a giant magnetostriction actuator for high power applications[C]//*Proceedings of the Power Conversion*, Osaka, Japan, April 25, 2002: 1102–1107.
4. TONG D, VELDHUIS S C. ELBESTAWI M A. Control of a dual stage magnetostrictive actuator and linear motor feed drive system [J]. *International Journal of Advanced Manufacturing Technology*, 2007, 33(3–4): 379–388.
5. LV Fuzai, XIANG Zhaiqin, QI Zongjun, et al. The mechanical design of micro displacement actuator for precision noncircular cutting[J]. *Mechanical Science and Technology*, 2000, 19(5): 767– 769. (in Chinese)
6. KIM J, DOO J. Magnetostrictive self-moving cell linear motor[J]. *Mechatronics*, 2003, 13 (7): 739–753.
7. LUO Y H, HUTAPEA P. Stress-strain behavior of a smart magnetostrictive actuator for a bone transport device[J]. *Journal of Medical Device*, 2008, 2(4): 041002-1.
8. LIU H F, WANG S J, MA C, et al. Study on an actuator with giant magnetostrictive aterials for driving galvanometer in selective laser intering precisely[J]. *International Journal of Mechatronics and Manufacturing Systems*, 2015, 9(3/4): 116–133.
9. XING Haiyan, DANG Yongbin, WANG Ben, et al. Quantitative metal magnetic memory reliability modeling for welded joints[J]. *Chinese Journal of Mechanical Engineering*, 2016, 29(2): 372–377.
10. LIU Changhai, JIANG Hongzhou. Influence of magnetic reluctances of magnetic elements on servo valve torque motors[J]. *Chinese Journal of Mechanical Engineering*, 2016, 29(1): 136–144.
11. ZHANG Peng, LEE Kwang-Hee, LEE Chul-Hee. Friction behavior of magnetorheological fluids with different material types and magnetic field strength[J]. *Chinese Journal of Mechanical Engineering*, 2016, 29(1): 84–90.
12. DAVINO D, GIUSTINIANI A, VISONE C. Compensation of magnetostrictive Hysteresis by Arduino: Floating versus fixed-point performances[J]. *IEEE Transactions on Magnetics*, 2014, 50, 11, Article number: 6971449.
13. LINNEMANN K, KLINKEL S, WAGNER W. A constitutive model for magnetostrictive and piezoelectric materials[J]. *International Journal of Solids and Structures*, 2009, 46 (5): 1149–1166.
14. LI Y S, ZHU Y C, WU H T. Modeling and inverse compensation for giant magnetostrictive transducer applied in smart material electrohydrostatic actuator[J]. *Journal of Intelligent Material Systems and Structures*, 2014, 25 (3): 378–388.
15. ZHU Yu-Chuan, XU Hong-Xiang, CHEN Long, et al. Dynamic preisach model in giant magnetostrictive actuator based on hyperbolic tangent function hysteresis operators[J]. *Journal of Mechanical Engineering*, 2014, 50(6): 165–170. (in Chinese)
16. MOSES A J, ANDERSON P I, SOMKUN S. Modeling 2-d magnetostriction in nonoriented electrical steels using a simple magnetic domain model[J]. *IEEE Transactions on Magnetics,* 2015, 51(5): 7036108.
17. ZHANG L X, WANG X S, CAO J. Measurement and compensation of pitch error based on GMA with elimination of its hysteresis[J]. *Journal of Mechanical Science and Technology*, 2014, 28(5): 1855–1866.
18. BERGQVIST A, ENGDAHL G. A stress-dependent magnetic preisach hysteresis model[J]. *IEEE Transactions on Magnetics*, 1991, 27 (6): 4796–4798.
19. TAN X B, BARASA J S. Modeling and control of hysteresis in magnetostrictive actuators[J]. *Automatica*, 2004, 40(9): 1469–1480.
20. HU C C, SHI Y G, CHEN Z Y. Synthesis, magnetic properties and magnetostriction of Pr0.5Nd0.5(Fe1-xCox)(1.9) cubic Laves alloys [J]. *Journal of Alloys and Compounds*, 2014, 613: 153–156.
21. LIU Huifang, JIA ZhenYuan, WANG Fuji, et al. Parameter indentification of displacement model for giant magnetostrictive actuator[J]. *Journal of Mechanical Engineering*, 2010, 46(15), 148–153. (in Chinese)
22. ZENG Jiewei, SU Lanhai, XU Liping, et al. Research on the stress measurement of steel plate based on inverse magnetostrictive effect [J]. *Journal of Mechanical Engineering*, 2014, 50(8): 17–22. (in Chinese)

Huifang LIU, born in 1983, is currently a lecturer in *School of Mechanical Engineering*, *Shenyang University of Technology*, *China*. She received her PhD degree in biotechnology from *Dalian University of Technology*, *China*, in 2012. Her main research fields are sensors, micro actuators, magnetostrictive materials and its application.E-mail: hfliu@sut.edu.cn

Xingwei SUN, born in 1970, is a professor and a master candidate supervisor at *School of* Mechanical *Engineering*, *Shenyang University of Technology*. She received her PhD degree in biotechnology from *Tianjin University*, *China*. Her main research fields are NC manufacturing technology of complex surface and functional materials.E-mail: sunxingw@126.com

Yifei GAO, born in 1984, is currently a lecturer at *School of Mechanical Engineering*, *Shenyang University of Technology*. He received her PhD in Biotechnology from *Dalian University of Technology*, *China*, in 2014. His main research fields are Multi-dimensional force measuring technology.E-mail: gaoyf2008@hotmail.com

Hanyu WANG, born in 1991, is a doctoral student of *Shenyang University of Technology*. His research interest is smart material and its application.Email: 18802408921@163.com

Zijin GAO, born in 1993, is an undergraduate of *Shenyang University of Technology*. His research interest is magnetostrictive driving technology.Email: zy_sut@163.com